Novel role for ALCAM in lymphatic network formation and function

Maria Iolyeva, Sinem Karaman, Ann-Helen Willrodt, Stephanie Weingartner, Benjamin Vigl, and Cornelia Halin[1]

Institute of Pharmaceutical Sciences, Swiss Federal Institute of Technology, ETH Zurich, Zurich, Switzerland

ABSTRACT **Adhesion molecules play an important role in vascular biology because they mediate vascular stability, permeability, and leukocyte trafficking to and from tissues. Performing microarray analyses, we have recently identified activated leukocyte cell adhesion molecule (ALCAM) as an inflammation-induced gene in lymphatic endothelial cells (LECs). ALCAM belongs to the immunoglobulin superfamily and engages in homophilic as well as heterophilic interactions. In this study, we found ALCAM to be expressed at the protein level in human and murine lymphatic and blood vascular endothelial cells *in vitro* and in the vasculature of human and murine tissues *in vivo*. Functional *in vitro* experiments revealed that ALCAM mediates adhesive interactions, migration, and tube formation in LECs, suggesting a role for ALCAM in lymphatic vessel (LV) stability and in lymphangiogenesis. Furthermore, ALCAM supported dendritic cell (DC) adhesion to lymphatic endothelium. In agreement with these findings, experiments performed in ALCAM$^{-/-}$ mice detected reduced LEC numbers in various tissues and defects in the formation of an organized LV network. Moreover, DC migration from lung to draining lymph nodes was compromised in ALCAM$^{-/-}$ mice. Collectively, our data reveal a novel role for ALCAM in stabilizing LEC-LEC interactions and in the organization and function of the LV network.—Iolyeva, M., Karaman, S., Willrodt, A.-H., Weingartner, S., Vigl, B., Halin, C. Novel role for ALCAM in lymphatic network formation and function. *FASEB J.* 27, 978–990 (2013). www.fasebj.org**

Key Words: adhesion molecule · lymphangiogenesis · dendritic cell migration

Abbreviations: ALCAM, activated leukocyte cell adhesion molecule; BEC, blood endothelial cell; BV, blood vessel; CAR, coxsackie and adenovirus receptor; CNS, central nervous system; DC, dendritic cell; dLN, draining lymph node; dMLN, draining mediastinal lymph node; EBM, endothelial basal medium; FBS, fetal bovine serum; GFP, green fluorescent protein; ICAM-1, intercellular adhesion molecule 1; Ig, immunoglobulin; JAM, junctional adhesion molecule; LEC, lymphatic endothelial cell; LN, lymph node; LV, lymphatic vessel; SLO, secondary lymphoid organ; VCAM-1, vascular cell adhesion molecule 1; WT, wild-type

CELL ADHESION MOLECULES expressed in blood vessels (BVs) are important for vascular development, control of vessel stability and vascular permeability, and also regulate leukocyte extravasation into tissues (1, 2). During pathological conditions like tumor growth, various vascular adhesion molecules, such as ESAM (3), $\alpha_v\beta_3$ integrin (4), or CD146 (5), have been shown to participate in vascular remodeling and angiogenesis. Intriguingly, many adhesion molecules expressed in the vasculature, *e.g.*, CD44, intercellular adhesion molecule 1 (ICAM-1), or members of the junctional adhesion molecule (JAM) family, are at the same time expressed on leukocytes and are also involved in immune function (1, 2).

Besides BVs, lymphatic vessels (LVs) constitute a second vascular network of the body (6). LVs begin as small, blind-ended capillaries in tissues. These funnel into collecting vessels and then into the thoracic duct, which eventually merges with the subclavian veins (6). LVs drain protein-rich fluid from tissues and return it to the blood vascular system. Furthermore, LVs play an important role in immunosurveillance: They mediate the migration of leukocytes, particularly of antigen-presenting dendritic cells (DCs), from peripheral tissues to lymph nodes (LNs), or from LNs back to the blood circulation (7). Finally, LVs are important for the uptake of dietary fats in the small intestine (6). LVs and BVs share many structural similarities: both vessel types are surrounded by a basement membrane and are composed of flattened endothelial cells that are interconnected by adhesion molecules like CD31, VE-cadherin, and members of the claudin and JAM families (6, 8). However, at the level of cell-cell junctions, marked differences exist between these two vessel types. While in BVs blood endothelial cells (BECs) are surrounded by a continuous lining of tight- and adherens-junction molecules, this arrangement is only found at the level of the collecting LVs. In initial lymphatic capillaries, neighboring oak leaf-shaped lymphatic endothelial

[1] Correspondence: Institute of Pharmaceutical Sciences, ETH Zurich, Wolfgang-Pauli Str. 10, HCI H413, CH-8093 Zurich, Switzerland. E-mail: cornelia.halin@pharma.ethz.ch

doi: 10.1096/fj.12-217844

This article includes supplemental data. Please visit *http://www.fasebj.org* to obtain this information.

0892-6638/13/0027-0978 © FASEB

cells (LECs) are loosely interconnected by discontinuous, button-like associations of junctional molecules (6). This characteristic setup of cell junctions gives rise to so-called primary valves or flaps between neighboring LECs, which are thought to represent the main entry sites for fluid and leukocytes into lymphatics (7, 9).

Recent studies have revealed that many adhesion molecules are essential for LV development and function. For example, the coxsackie and adenovirus receptor (CAR) was shown to be important for the development of LVs (10), whereas the integrin α_9 was shown to control lymphatic valve formation (11). Furthermore, integrin $\alpha_4\beta_1$ reportedly is involved in tumor lymphangiogenesis and in the metastatic spread of tumor cells to draining LNs (dLNs; ref. 12). Moreover, several studies have shown that in the presence of tissue inflammation, LECs—similarly to BECs—up-regulate the adhesion molecules ICAM-1 and vascular cell adhesion molecule 1 (VCAM-1), which participate in the migration of leukocytes to dLNs (7). However, at present, comparably little is known about the role of LEC-expressed adhesion molecules in lymphangiogenesis and LV function.

To identify new LEC-expressed adhesion molecules, we have recently performed a microarray-based gene expression analysis of primary human LECs cultured in presence or absence of the inflammatory cytokine TNF-α. One of the genes found to be up-regulated in response to TNF-α-treatment was activated leukocyte cell adhesion molecule (ALCAM; also known as CD166). ALCAM is an adhesion molecule of the immunoglobulin (Ig) superfamily with reported expression in certain epithelia, various leukocyte subsets (*i.e.*, monocytes, DCs, and activated T cells), and neurons. ALCAM contains 5 extracellular Ig domains, a transmembrane domain, and a short C-terminal cytoplasmic tail. It engages in homophilic ALCAM-ALCAM interactions, which are mediated by the N-terminal Ig domains of ALCAM molecules on neighboring cells. ALCAM-mediated adhesion is further strengthened by lateral oligomerization of neighboring molecules on the cell surface, which involves the more membrane-proximal Ig domains of the molecule (13). Besides homophilic interactions, ALCAM further engages in heterophilic interactions with the scavenger receptor CD6, which is expressed on virtually all T cells (14). Recently, heterophilic interactions of ALCAM with other molecules, such as L1CAM (15) or galectin-8 (16), also have been reported. Besides its function in the central nervous system (CNS), ALCAM has been implicated in diverse cellular processes, such as T cell activation (17), tumor invasion (18) and endothelial cell biology (19–22). In fact, ALCAM expression was recently reported in cultured BECs (20, 21) and in BVs in the lung, liver and CNS *in vivo* (22–24). ALCAM was shown to localize to cell-cell junctions in BECs (21) and to support tube formation of yolk sac–derived endothelial cells (19). Furthermore, ALCAM reportedly mediates the migration of ALCAM-expressing monocytes across inflamed blood vascular endothelium *in vitro* (21) and *in vivo* (22). By contrast, nothing is known about the expression and function of ALCAM in the lymphatic vascular system.

In this study, we have analyzed the expression of ALCAM in LECs *in vitro* and *in vivo*. Our data confirmed expression of ALCAM in cultured human dermal LECs and demonstrated that ALCAM promotes LEC migration and tube formation and also strengthens LEC interactions with other ALCAM-expressing cells. Furthermore, experiments in wild-type (WT) and $ALCAM^{-/-}$ mice confirmed the expression of ALCAM in LVs and in BVs *in vivo* and revealed phenotypic and functional abnormalities in LVs of $ALCAM^{-/-}$ mice. Overall, our data point toward a new role for ALCAM in the organization of the LV network and in LV function.

MATERIALS AND METHODS

Cell culture

Human LECs were isolated from neonatal human foreskins as described previously (25). Cells were cultured on plates coated with collagen type I (Advanced BioMatrix, Poway, CA, USA; 3.1 mg/ml) and fibronectin (Millipore, Billerica, MA, USA; 1 mg/ml) in endothelial basal medium (EBM; Lonza, Walkersville, MD, USA) supplemented with 20% fetal bovine serum (FBS; Gibco, Paisley, UK), antibiotic antimycotic solution (Fluka, Buchs, Switzerland), L-glutamine (2 mM; Fluka), hydrocortisone (10 μg/ml; Fluka), and N^6,2′-O-dibutyryladenosine 3′,5′-cyclic monophosphate sodium salt (cAMP, 25 μg/ml; Fluka). Cells were grown at 37°C in presence of 5% CO_2 and cultured for up to 10 passages. In some assays, LECs were stimulated with TNF-α and IFNγ (20 ng/ml each; PeproTech, Rocky Hill, NJ, USA), and cells were analyzed after 24–48 h.

Generation of human monocyte-derived DCs

Peripheral blood cells were isolated from buffy coats obtained from healthy donors (Blutspende Zürich, Zurich, Switzerland). Polymorphonuclear cells were isolated by density centrifugation with Ficoll-Paque Plus (GE Healthcare, Stockholm, Sweden), followed by incubation with ACK buffer to lyse erythrocytes. Monocytes were isolated from polymorphonuclear cells by magnetic-activated cell sorting (MACS) using an anti-human CD14 kit (Miltenyi Biotech, Gladbach, Germany). Cells were cultured at 37°C in the presence of 500 U/ml of human GM-SCF (PeproTech) and 500 U/ml of human IL-4 (R&D Systems, Abingdon, UK). Fresh medium was added on d 4 of culture. On d 8, the floating cell fraction was harvested, and DCs were activated overnight with 100 ng/ml of LPS (Alexis Biochemicals, Lausen, Switzerland). On d 9, DCs were used in the DC-LEC adhesion assay. Monocyte and DC purity and activation status was analyzed by FACS using the following antibodies: anti-human CD14-FITC, anti-human CD11c-PE, anti-human CD86-FITC, anti-human CD80-FITC, and the corresponding isotype controls (all from BD Biosciences, Basel, Switzerland). DC purity generally was >90%.

FACS analysis of cultured cells and of single-cell suspensions generated from murine tissues

In vitro cultured human LECs were washed with PBS and detached by treatment with Accutase (Sigma-Aldrich, Gilling-

ham, UK). Human monocyte-derived DCs were collected and washed with PBS before FACS staining. Antibody incubations were performed on ice in PBS containing 1% FBS using the following antibodies: mouse anti-human ALCAM and mouse anti-human ICAM-1 (both from R&D Systems). PE-conjugated secondary antibodies (Caltag Laboratories, Little Balmer, UK) were used for detection.

To obtain single-cell suspensions, mouse tissues were digested with collagenase IV (Invitrogen, Basel, Switzerland) and subsequently passed through a 40-μm cell strainer (Invitrogen), as described previously (26). Cell suspensions were stained with anti-mouse CD31-APC, anti-mouse CD45-PerCP, anti-mouse CD11c-APC, anti-mouse CD103-PE, anti-mouse MHCII (IA-IE)-PerPC, anti-mouse CD11b-FITC, anti-mouse Gr1-PE, anti-mouse CD4-PE, anti-mouse CD8a-FITC, anti-mouse CD3ε-APC, anti-mouse B220-PerCP-Cy5.5 (all from BioLegend, San Diego, CA, USA), hamster anti–mouse podoplanin (clone 8.1.1, Developmental Studies Hybridoma Bank, University of Iowa, Iowa City, IA, USA), and anti-hamster-PE (Invitrogen) or anti-hamster-Alexa488 (Invitrogen). The cellularity of LNs, spleen, and thymus was determined manually using a cell counting chamber. Total cell numbers in ear or lung samples were determined by FACS, using counting beads (Invitrogen). In each case, a defined aliquot of the sample was stained and acquired by FACS. The expression of ALCAM was detected by additionally staining with goat-anti-mouse ALCAM (R&D Systems) and the corresponding Alexa488- or PE-labeled secondary antibodies (Invitrogen). FACS data were acquired on a BD FACSCanto (BD Biosciences) using FACSDiva software (BD Bioscience). Data were analyzed offline using FlowJo software (Treestar, Ashland, TN, USA). In some experiments, ΔMFI values, defined as the difference in the median fluorescent intensity between the candidate and the corresponding isotope control staining, were calculated.

Tube formation assay

Confluent LEC monolayers grown in 24-well plates were cultured for 24 h in starvation medium (EBM supplemented with 2% FCS and antibiotic antimycotic solution). Subsequently, wells were overlaid with 0.5 ml of neutralized isotonic bovine dermal collagen type I (1 mg/ml; Advanced BioMatrix) containing 10 μg/ml of either anti-human-ALCAM blocking antibody, human ALCAM-Fc, or the corresponding IgG control (all from R&D Systems). Representative images (3/well) of the tubes were captured after 16–18 h, and the total length of all tube-like structures in the pictures of each well was measured using an ImageJ-based script developed in-house.

Scratch-wound assay

Confluent LEC monolayers grown in 24-well plates were cultured for 24 h in starvation medium. Subsequently, two cross-shaped scratches were made in each well, using a pipette tip. Monolayers were washed with PBS, and 500 μl of starvation medium supplemented with anti-human-ALCAM blocking antibody, IgG control (10 μg/ml; both from R&D Systems), or VEGF-A (20 ng/ml; PeproTech) was added. Pictures were taken immediately after scratching and 16–24 h later. For each cross (8–10/condition), the percentage of the surface area closed after 16–24 h was calculated, using T-scratch software (27).

Adhesion assay

LECs (10^4 cells/well) were seeded into a 96 well plate (black-walled, clear-bottom, Costar, Corning Inc., Lowell, MA, USA) and grown to confluence. At this point, LECs grown in separate culture dishes were labeled with calcein (Calcein AM; Invitrogen), detached with Accutase (Sigma-Aldrich), washed with PBS, and resuspended in complete medium. For the DC-LEC adhesion assay, human monocyte-derived DCs were labeled with calcein, washed with PBS, and resuspended in DC medium. For both assays (DC-LEC and LEC-LEC adhesion), 10^4 fluorescently labeled cells were added to the wells of the 96-well plate (8–12 wells/condition). Experiments were performed in the presence of anti-human-ALCAM blocking antibody, human ALCAM-Fc, or of the corresponding IgG control (10 μg/ml; all from R&D Systems). After 1 h of incubation at 37°C, the wells were washed with PBS and trypsinized, and the numbers of calcein-labeled adherent cells were quantified by FACS.

Mice

WT C57BL/6J mice were purchased from Charles River Laboratories (Sulzbach, Germany). ALCAM$^{-/-}$ mice (28) on a C57BL/6J background were obtained from Jackson Laboratories (Bar Harbor, ME, USA). All mice were bred and housed in our specific and opportunistic pathogen-free (SOPF) mouse facility. All experiments were approved by the Cantonal Veterinary Offices of Zurich.

Immunofluorescence analysis of human tonsil and skin and mouse LN

Immunofluorescence analyses of tissue sections were performed as described previously (26). In brief, sections were incubated for 2 h at room temperature with the following primary antibodies in antibody diluent (Zytomed Systems, Berlin, Germany): goat-anti-mouse ALCAM (R&D Systems), rabbit anti-mouse LYVE-1 (AngioBio, Del Mar, CA, USA), rabbit-anti-green fluorescent protein (GFP; Invitrogen), rat-anti-mouse CD45R/B220 (BD Biosciences), mouse-anti-human CD31 (Dako, Glostrup, Denmark), rabbit-anti-human LYVE-1 (TECOmedical Group, Sissach, Switzerland). Alexa488- or Alexa594-coupled secondary antibodies (Invitrogen) were used for detection. Slides were mounted with Vectashield mounting medium (Vector Laboratories, Burlingame, CA, USA) and examined using an Axioskop 2 MOT plus microscope equipped with 20/0.50 Plan-Neofluar, 40/1.3 oil Plan-Neofluar, and 63/1.25 oil Plan-Neofluar objectives and an AxioCam MRm monochrome digital camera (all from Carl Zeiss AG, Feldbach, Switzerland). Images were acquired using AxioVision 4.4 software (Carl Zeiss). Adobe Photoshop CS2 (Adobe Systems, San Jose, CA, USA) was used for image processing.

Immunoblotting analysis

LEC monolayers were stimulated with TNF-α and IFNγ (20 ng/ml each; PeproTech) or PBS control. After 24 h, total protein was extracted into lysis buffer (20 mM Tris, 150 mM sodium chloride, 5 mM EDTA, 1% Triton X, 25 mM sodium fluoride, 1 mM PMSF, 10% glycerol, and Complete Mini, EDTA-free protease inhibitor; Roche, Basel, Switzerland). Next, 50 μg of total protein was separated on a 10% separating acrylamide gel and transferred onto a nitrocellulose membrane (Bio-Rad, Hercules, CA, USA). Immunoblotting was performed using mouse-anti-human ALCAM (R&D Systems) and rabbit-anti-human p44/42 MAPK (Erk1/2; Cell Signaling, Boston, MA, USA), followed by incubation with HRP-conjugated secondary antibodies (Zymed Laboratories; Invitrogen). Protein bands were visualized using the ECL plus Western blotting detection system (GE Healthcare), and

X-ray films (Super RX Fujifilm; LucernaChem, Lucerne, Switzerland) were developed on an AGFA Curix 60 film processor (AGFA, Morstel, Belgium).

In vivo lung DC migration assay

Fluoresbrite yellow green microspheres (0.5 μm diameter; Polysciences, Warrington, PA, USA) were diluted to 1:5 v/v in PBS. ALCAM$^{-/-}$ and WT mice were anesthetized by inhalation of isoflurane (Attane; Minrad Inc., Buffalo, NY, USA), and 50 μl of microspheres (3.64×10^9 microspheres) was administered intratracheally. After 24 h, lung draining mediastinal LNs (dMLNs) were harvested, and single-cell suspensions were generated by passaging through a 40-μm cell strainer (BD Biosciences). Samples were stained with anti-CD11c-APC, anti-I-A/I-E (MHCII)-PerCP, and anti-CD103-PE (all from BioLegend). The number of FITC$^+$CD11c$^+$IA/IE$^+$ DCs per LN was quantified by FACS analysis with the help of counting beads (Invitrogen).

Whole-mount staining

Intestines with attached mesentery or diaphragms were collected from P6 mice and fixed in 4% paraformaldehyde in PBS. Tissues were blocked and permeabilized by incubation in 1% BSA, 0.05% sodium azide, 0.01% Triton-X, and 5% normal donkey serum (Sigma-Aldrich) in PBS for 1 h. The following antibodies were used: rabbit anti Prox-1 (a kind gift from K. Alitalo, University of Helsinki, Helsinki, Finland; ref. 29), PECAM-1 (BD Bioscience) rabbit anti-mouse LYVE-1 (AngioBio), and rat anti-mouse MECA-32 (BD Bioscience); and AlexaFluor 488-, 594-, or 647-conjugated secondary antibodies (all from Invitrogen). Samples were mounted with Vectashield (Vector Laboratories) on chambered cover glasses (Nunc, Rochester NY, USA) for confocal imaging. Whole-mount *z* stacks were acquired using an LSM 710 FCS confocal microscope equipped with a 10/0.3 EC Plan-Neofluar objective using ZEN software (Zeiss) and processed with Imaris software (Bitplane AG, Zürich, Switzerland). Computer-assisted quantification of LV parameters in the mesentery was performed by tracing Prox-1 staining of 3 mesenteric attachments per mouse, and LYVE-1 staining of 1 diaphragm window per mouse. The total LV area was determined using an area-calculating tool. The total length of LVs and the number and distance between branching points was measured using ImageJ. The average LV diameter was calculated by dividing the area with the vessel length. The numbers of branching points, valves, lymphatic rings, and blind-ended LVs were quantified manually.

Statistical analysis

Data were analyzed using the Student's *t* test (unpaired, 2-tailed, or paired when indicated) and are presented as means ± SE. Differences were considered statistically significant at values of $P < 0.05$.

RESULTS

ALCAM is expressed in human LECs *in vitro* and *in vivo*

To investigate the expression of ALCAM at the protein level, we performed FACS analysis on *in vitro* cultured human dermal LECs. This analysis confirmed ALCAM expression on the LEC cell surface (**Fig. 1*A*, *B***). Similar to ICAM-1, ALCAM expression was further up-regu-

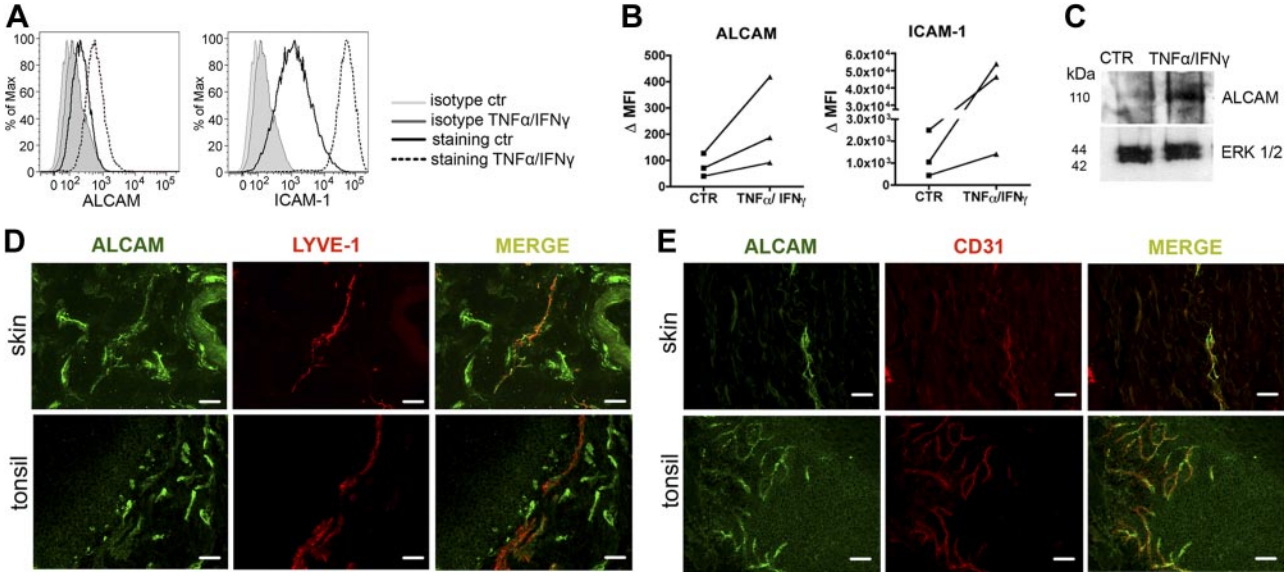

Figure 1. ALCAM is expressed on human LECs *in vitro* and *in vivo*. *A*, *B*) FACS analysis revealed that *in vitro* cultured LECs express ALCAM at steady state, and that its expression is up-regulated on overnight treatment with TNF-α and IFNγ (each 20 ng/ml). *A*) Representative histogram plots showing that cytokine-treatment induced an increase in the expression of ALCAM and of ICAM-1 (positive control). Black solid trace: control staining. Black dashed trace: TNF-α/IFNγ treatment. Gray shaded trace: isotype controls. Representative plots from three different experiments are shown. *B*) Summary of the ΔMFI values measured in all experiments. *C*) Immunoblotting analysis performed on LEC protein extracts with ALCAM-pecific antibodies detected a band of ~110 kDa, corresponding to the molecular weight of human ALCAM protein, which was further induced by treatment of LECs with TNF-α and IFNγ. Protein levels of ERK1/2 were analyzed as loading control. *D*, *E*) Immunofluorescence analysis of human skin and tonsil sections. In both tissues. ALCAM expression was detected in LYVE-1$^+$ LVs (*D*) as well as in all vascular structures, as evidenced by costaining with the endothelial-specific marker CD31$^+$ (*E*). Scale bars = 50 μm.

lated on treatment with the inflammatory cytokines TNF-α and IFNγ. Western blot analysis performed on LEC protein extracts detected a band of ~110 kDa, corresponding to the described molecular weight of membrane-bound ALCAM (21), which was induced on cytokine treatment (Fig. 1*C*). To validate the expression of ALCAM in LVs *in vivo*, immunofluorescence was performed on tissue sections generated from human skin and tonsils (Fig. 1*D*, *E*): ALCAM expression was detected in LYVE-1$^+$ LVs in both tissues. In addition, costaining with the panendothelial marker CD31 revealed a complete colocalization between ALCAM and CD31, indicating that ALCAM was expressed in both LVs and BVs of human skin and tonsils (Fig. 1*D*, *E*).

ALCAM mediates LEC adhesion, migration, tube formation, and interaction with DCs

Since ALCAM is known to engage into homophilic interactions (14) and to localize to endothelial cell junctions (21), we performed functional *in vitro* assays to investigate whether ALCAM-ALCAM interactions could be important for LEC biology. In a first experiment, we investigated the role of ALCAM in a scratch-wound assay. To this end, scratches were introduced into confluent LEC monolayers, and the migration of bordering LECs into the cell-free zones of the scratches was evaluated 24 h later. While the addition of VEGF-A to the assay significantly enhanced LEC migration and scratch closure, this process was significantly reduced in presence of an ALCAM-blocking antibody, as compared to the corresponding isotype control IgG (−27%, P=0.019; **Fig. 2*A*, *B***). Similarly, blockade of ALCAM significantly impaired VEGF-A-induced scratch closure (−51%, P=0.008; Fig. 2*C*). In the next step, we investigated whether blockade of ALCAM would affect the ability of cultured LECs to form tube-like structures *in vitro*. Indeed, when performing this assay in the presence of an ALCAM-blocking antibody, tube formation into collagen gels was significantly reduced (−23%, P=0.006; Fig. 2*D*, *E*). Similarly, tube formation was reduced in presence of a fusion protein consisting of the extracellular domains ALCAM and the Fc portion of an IgG antibody (−39% P<0.0001, respectively; Fig. 2*D*, *E*). The latter is thought to bind to and to block LEC-expressed ALCAM by forming homophilic interactions. Finally, we studied whether ALCAM was important for adhesive interactions between neighboring LECs. To this end, LECs were grown to confluence and incubated with cell suspensions of fluorescently labeled LECs. Addition of an ALCAM-blocking antibody significantly reduced the adhesion of labeled LECs to LEC monolayers (−38%, P<0.0001; Fig. 2*F*). Notably, similar results were obtained when performing adhesion assays with murine conditionally immortalized murine LECs (30) in presence of murine ALCAM-Fc, indicating a similar role for ALCAM in the murine system (data not shown). *In vivo*, LECs engage in cell-cell interactions with other LECs or stromal cells. Furthermore, LECs interact with leukocytes, which use LVs for their migration to dLNs. Interestingly, ALCAM expression was recently reported for human monocyte-derived DCs and to contribute to T cell activation by binding to the T cell-expressed costimulatory molecule CD6 (17). In agreement with the latter report, we detected ALCAM expression in human peripheral blood monocyte-derived DCs (Fig. 2*G*). We next investigated whether blockade of ALCAM would affect DC-LEC interactions *in vitro*. Indeed, inhibition of ALCAM with a blocking antibody or with ALCAM-Fc fusion protein significantly reduced the adhesion of DCs to LEC monolayers (−26%, P=0.003, and −18%, P=0.02, respectively; Fig. 2*H*). In sum, our *in vitro* data suggested a role for ALCAM in LEC migration, tube formation, and the interactions between LECs or between LECs and DCs.

ALCAM is expressed by LECs and leukocytes in LNs and is important of LN homeostasis

To further study the role of ALCAM in LEC biology, we turned to investigating the expression of ALCAM in mice. Surprisingly, when performing FACS analysis on enzymatically digested mouse ear skin, ALCAM expression was detected on some skin-resident leukocytes but not on LECs or BECs (data not shown). Similarly, we could not detect ALCAM expression in LVs or BVs by immunofluorescence performed on murine skin sections (data not shown). However, FACS analysis performed on single-cell suspensions generated from murine LNs detected high levels of ALCAM in LECs and in leukocytes, whereas lower ALCAM levels were expressed in BECs (**Fig. 3*A*, *B***).

ALCAM-deficient mice were generated several years ago (28). These mice were originally described to have axon fasciculation defects and retinal dysplasias, but otherwise did not display any gross physical or behavioral abnormalities (28). Since ALCAM$^{-/-}$ mice have thus far not been analyzed with regard to a potential vascular phenotype, we investigated the LV network in various organs of these mice. In the first step, we analyzed the LN vasculature in ALCAM$^{-/-}$ as compared to WT mice. FACS analysis confirmed that ALCAM was exclusively expressed in LN LECs from WT, but not from ALCAM$^{-/-}$ mice (Supplemental Fig. S1*A*, *B*). Since in ALCAM$^{-/-}$ mice the ALCAM gene was disrupted by the insertion of a cDNA encoding for green fluorescent protein GFP (28), it is possible to analyze GFP expression as a reporter for ALCAM promoter activity. Indeed, immunofluorescence performed on LN sections of ALCAM$^{-/-}$ mice detected GFP expression in LYVE-1$^+$ lymphatic structures (Supplemental Fig. S1*C*). In agreement with these findings, immunofluorescence performed on LN sections from WT mice revealed a colocalization between LYVE-1$^+$ LV structures and ALCAM staining, whereas no staining for ALCAM was detected on LYVE-1$^+$ LV structures in LNs of ALCAM$^{-/-}$ mice (Fig. 3*C*). Notably, besides LVs, other structures (presumably leukocytes) also stained positive for ALCAM in LNs from WT but not from

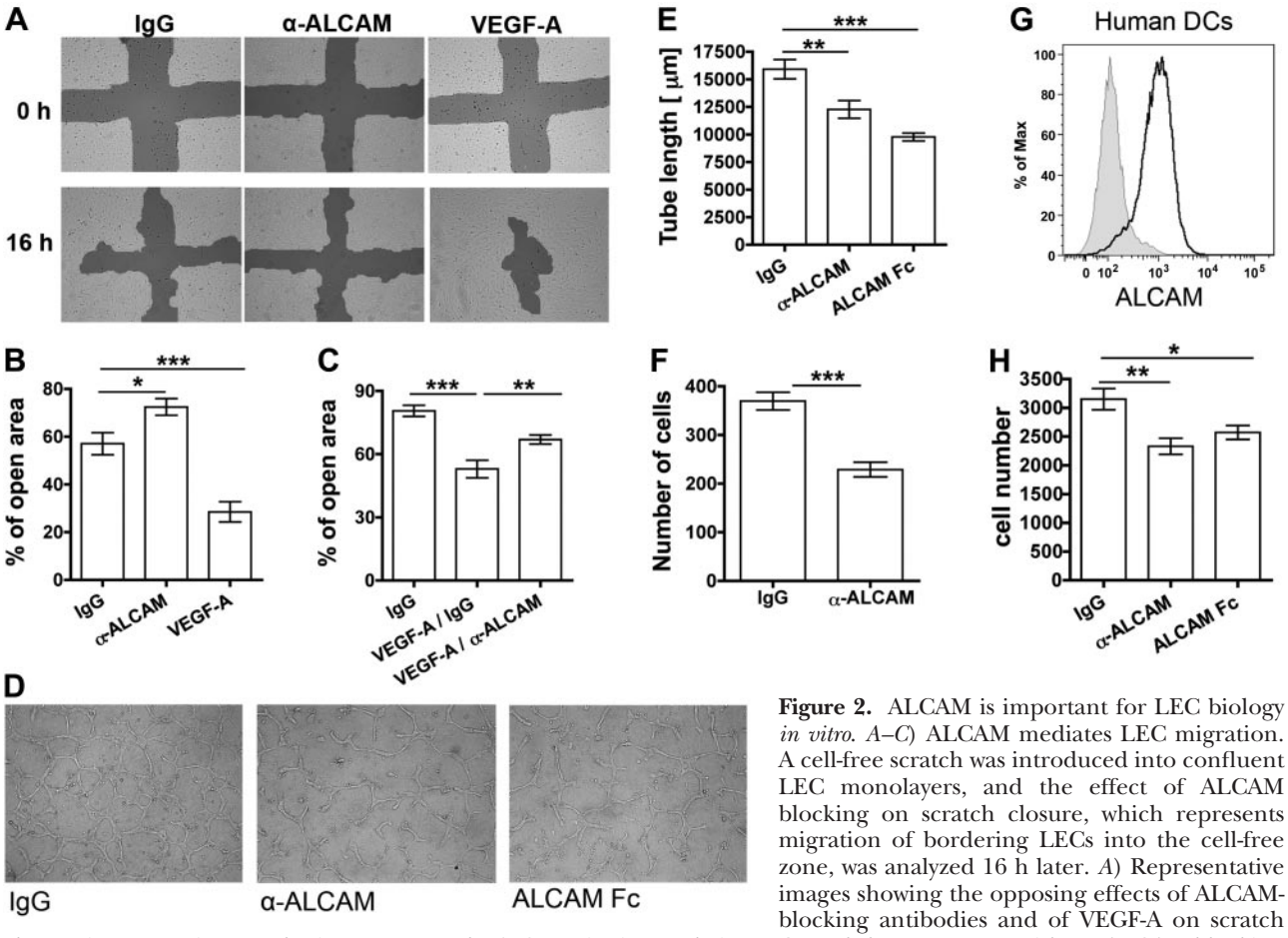

Figure 2. ALCAM is important for LEC biology *in vitro*. *A–C*) ALCAM mediates LEC migration. A cell-free scratch was introduced into confluent LEC monolayers, and the effect of ALCAM blocking on scratch closure, which represents migration of bordering LECs into the cell-free zone, was analyzed 16 h later. *A*) Representative images showing the opposing effects of ALCAM-blocking antibodies and of VEGF-A on scratch closure in comparison to the isotype control. *B*) Quantitative analysis confirmed that treatment with an ALCAM-blocking antibody significantly reduced scratch closure, whereas treatment with VEGF-A accelerated the scratch closure. *C*) Moreover, ALCAM blockade significantly reduced VEGF-A-induced scratch closure. *D, E*) ALCAM mediates LEC tube formation. Tube formation assays were performed by covering confluent LEC monolayers with collagen type I containing ALCAM blocking antibodies, ALCAM-Fc, or isotype control antibody. Treatment with an ALCAM-blocking antibody or with ALCAM-Fc fusion protein reduced tube-formation capacity of LECs. *D*) Representative images. *E*) Quantitative analysis. *F*) Blocking ALCAM with a specific antibody reduced adhesion of LECs to LEC monolayers in comparison to the isotype control. *G, H*) ALCAM mediates the adhesion of DCs to LEC monolayers. *G*) DCs were generated from human blood-derived monocytes, and the expression of ALCAM was analyzed by FACS. *H*) Treatment with an ALCAM-blocking antibody or with ALCAM-Fc fusion protein significantly reduced the ability of DCs to adhere to LECs monolayers. Results from one of 2–3 similar experiments are shown. $*P < 0.05$; $**P < 0.01$; $*** P < 0.001$.

ALCAM$^{-/-}$ mice (Fig. 3*C*). When further analyzing the phenotype of LNs of ALCAM$^{-/-}$ mice, we found that all skin dLNs analyzed (*i.e.*, axial, brachial, inguinal) were significantly reduced in weight (−35%, P=0.02; Fig. 3*D*) and in cellularity (−32–44%; Fig. 3*E*) as compared to LNs from WT control mice. The decrease in LN cellularity was paralleled by a proportional decrease in the number of CD45$^+$ cells (−33%, P=0.005; Fig. 3*F*). Interestingly, when quantifying LECs and BECs in these LNs by FACS we observed that LEC but not BEC numbers were significantly reduced in ALCAM$^{-/-}$ mice (−29%, P=0.02; Fig. 3*G*), in agreement with higher ALCAM expression in LECs than in BECs (Fig. 3*B*). Immunofluorescence of LN sections did not reveal any gross changes in LN architecture and segmentation into B-cell zones or T-cell areas (Fig. 3*H* and data not shown).

To further characterize the immune phenotype of ALCAM$^{-/-}$ mice, the leukocyte composition of the spleen, LNs, and thymus was analyzed (**Fig. 4*A–F***). These experiments revealed that CD4$^+$ and CD8$^+$ T cells, B cells, DCs, neutrophils, and macrophages were reduced in the LNs of ALCAM$^{-/-}$ mice (Fig. 4*B, C*). By contrast, leukocyte numbers in the spleen were similar in ALCAM$^{-/-}$ and WT mice (Fig. 4*D, E*). Thus, ALCAM deficiency did not lead to a general reduction of leukocytes in secondary lymphoid organs (SLOs), suggesting that the reduction in LN cellularity could be linked with the lymphatic phenotype observed in ALCAM$^{-/-}$ mice. Interestingly, in the thymus, the number of single-positive CD4$^+$ and CD8$^+$ thymocytes was significantly reduced (Fig. 4*F*).

ALCAM is expressed in the lung vasculature and is important for DC migration

We next analyzed whether ALCAM was expressed in LVs in other tissues. Indeed, FACS analysis performed

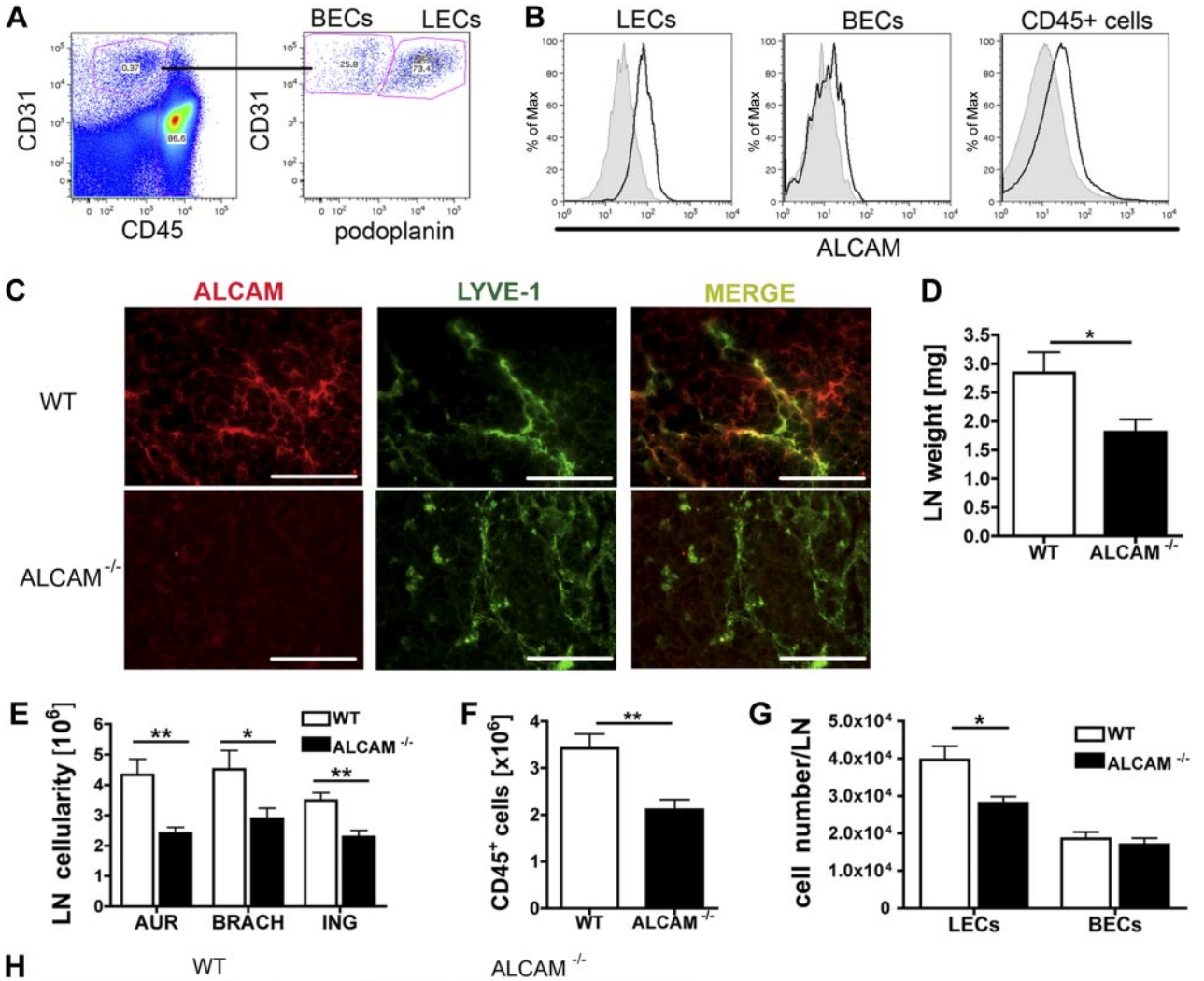

Figure 3. ALCAM is expressed on lymphatic vessels and leukocytes in murine LNs and is important for LN homeostasis. *A*, *B*) To investigate the expression of ALCAM in murine LNs, single-cell suspensions generated from enzymatically digested mouse LNs were stained with antibodies against CD45, CD31, podoplanin, and ALCAM to differentiate by FACS analysis between LECs ($CD45^-CD31^+podoplanin^+$), BECs ($CD45^-CD31^+podoplanin^-$), and leukocytes ($CD45^+CD31^-podoplanin^-$). *A*) Gating Scheme. *B*) Analysis revealed that ALCAM was expressed at high levels in LECs and $CD45^+$ cells but only at low levels in BECs. Black trace: candidate gene. Gray shaded trace: isotype control. *C*) Immunofluorescence performed on LN sections from $ALCAM^{-/-}$ and from WT mice further confirmed expression of ALCAM on LYVE-1^+ lymphatic structures. *D–G*) Auricular, brachial, and inguinal LNs from $ALCAM^{-/-}$ and WT mice were analyzed. *D, E*) LNs of $ALCAM^{-/-}$ mice were significantly reduced in weight (*D*; all LNs), and in cellularity (*E*). AUR, auricular; BRACH, brachial; ING, inguinal. *F*) Moreover, significantly lower numbers of $CD45^+$ leukocytes were present in the LNs of $ALCAM^{-/-}$ mice in comparison to the LNs of WT control mice. Pooled data from two similar experiments are shown ($n=10$ mice/genotype; *D–F*). *G*) Furthermore, LEC but not BEC numbers were significantly reduced in LNs from $ALCAM^{-/-}$ mice. Results from one experiment (n=5 mice/genotype) out of 3 similar experiments are shown. *H*) Immunofluorescence analysis of LYVE-1 and B220 expression in the mouse LN sections revealed no gross differences in the LN architecture in $ALCAM^{-/-}$ as compared to WT mice. Scale bars = 50 μm (*C*); 200 μm (*H*). $^*P < 0.05$; $^{**}P < 0.01$.

on single-cell suspensions generated from enzymatically digested mouse lungs detected ALCAM expression in both LECs and BECs and, to a lower degree, in lung-resident leukocytes (**Fig. 5*A*, *B***). The FACS staining for ALCAM was again specific, since no ALCAM signal was detected when analyzing lungs of $ALCAM^{-/-}$ mice (Supplemental Fig. S1*D*, *E*). FACS-based quantification revealed that LEC and BEC numbers were significantly reduced in the lungs of $ALCAM^{-/-}$ mice as compared to WT mice (−59%, $P=0.024$, and −52%, $P=0.005$, respectively; Fig. 5*C*). By contrast, total numbers of $CD45^+$ leukocytes and of $CD11c^+$ DCs were

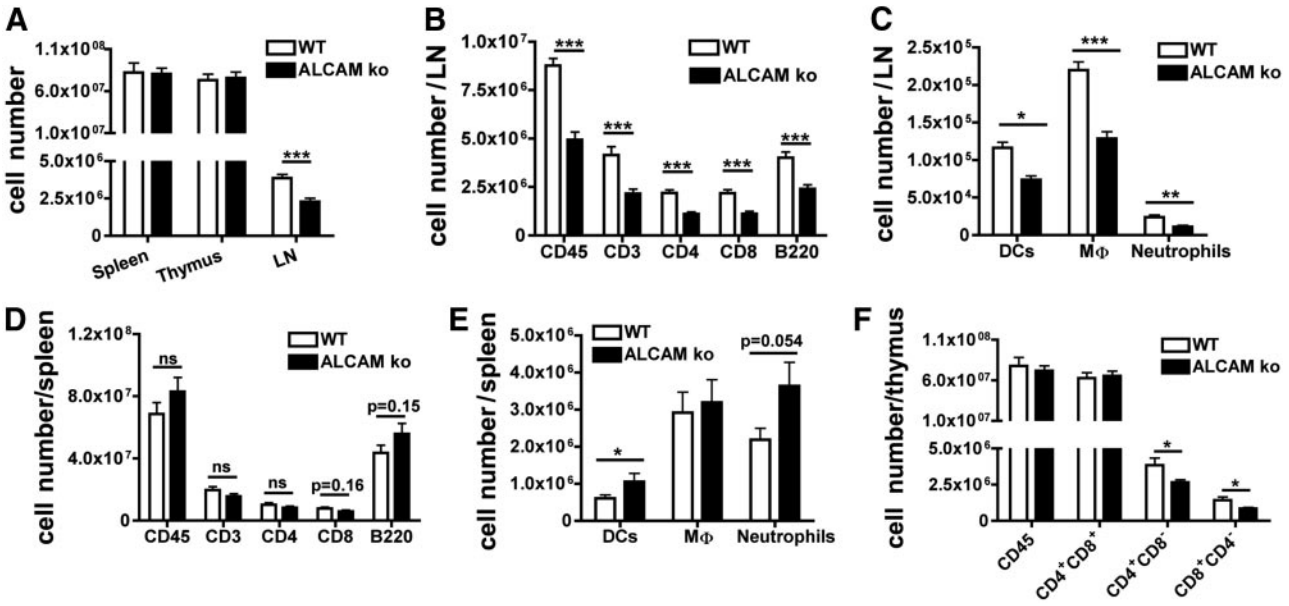

Figure 4. Analysis of the cellular composition of lymphoid organs in ALCAM$^{-/-}$ and WT mice. Spleen, thymus, and LNs were harvested, and single-cell suspensions were counted and analyzed by FACS. *A*) While the cellularity of skin dLNs (average LN cellularity obtained from pooled samples of axial, brachial, and inguinal LNs) was significantly reduced, no differences where observed in the cellularity of the spleen and thymus in ALCAM$^{-/-}$ as compared to WT mice. *B*, *C*) Quantitative FACS analysis revealed that all leukocyte subsets analyzed were significantly reduced in skin dLNs. *D*, *E*) In the spleen, no difference in lymphocyte numbers were observed (*D*), whereas DC and neutrophil counts were increased (E). *F*) In the thymus, the number of single-positive CD4$^+$CD8$^-$ and CD8$^+$CD4$^-$ thymocytes was significantly reduced. Cells were identified by the following combination of markers: DCs, CD11c$^+$; macrophages (MΦ), CD11b$^+$Gr1$^-$; neutrophils, CD11b$^+$Gr1$^+$. Pooled data from 2 similar experiments are shown (n=10 mice/genotype). *$P < 0.05$; **$P < 0.01$; ***$P < 0.001$.

similar in ALCAM$^{-/-}$ and in WT mice (Fig. 5*D*, *E*). Notably, no difference in the overall lung weight was found (data not shown). The reduction in LEC and BEC numbers indicated that vascular morphology and, possibly, function was altered in ALCAM$^{-/-}$ mice. To address whether LV function was compromised, DC migration experiments were performed, by intratracheally injecting FITC$^+$ fluorescent microbeads. These beads are too large to be passively drained into LVs, but are efficiently taken up and transported to dLNs by DCs (31). Similarly, as observed in skin dLNs, the lung dMLNs had a significantly reduced cellularity in ALCAM$^{-/-}$ as compared to WT mice (−49%, P=0.008, Fig. 5*F*). Quantitative FACS analysis revealed that CD11c$^+$ DCs were reduced in MLNs (−54.7%, P=0.055, Fig. 5*G*). When quantifying fluorescent microbead-positive (FITC$^+$) DCs in the dMLNs 24 h after bead injection, a distinct population of CD11c$^+$MHCII$^+$ FITC$^+$ DCs was visible in dMLNs of ALCAM$^{-/-}$ and WT mice (Fig. 5*H* and data not shown). Interestingly, the number of CD11c$^+$MHCII$^+$FITC$^+$ DCs recovered from dMLNs was significantly reduced in ALCAM$^{-/-}$ mice as compared to WT mice (−70%, P=0.0004, Fig. 5*I*). However, the percentage of CD11c$^+$MHCII$^+$FITC$^+$ DCs among all MLN cells was similar in both groups (Fig. 5*J*), indicating that the reduction in DC migration was proportionate to the LN cellularity. A more detailed analysis of lung-resident DCs revealed that ALCAM was highly expressed by CD103$^+$CD11c$^+$ DCs, whereas only a weak signal for ALCAM was detected in CD103$^-$CD11c$^+$ DCs (Supplemental Fig. S2*A*, *B*). Interestingly, DC migration from lung to dMLNs was similarly reduced for both ALCAM^{hi}CD103$^+$CD11c$^+$ and ALCAM^{lo}CD103$^-$CD11c$^+$ DCs (Supplemental Fig. S2*C*, *D*). This indicated that the reduction observed in *in vivo* DC migration in ALCAM$^{-/-}$ mice did not primarily depend on ALCAM expression by DCs or on the loss of ALCAM-ALCAM interactions between DCs and LECs.

ALCAM deficiency results in an abnormal organization of the LV network

To further characterize potential defects in the lymphatic vasculature of ALCAM$^{-/-}$ mice, we performed whole-mount analysis on mesenteries collected from 6-d-old (P6) pups. To this end, tissue was stained for the lymphatic-specific transcription factor Prox-1. In contrast to LYVE-1, which is expressed in lymphatic capillaries but is down-regulated in lymphatic collectors, Prox-1 is expressed by both vessel types (32). Notably, most LVs in the mesentery are collectors. Whole-mount analysis revealed marked differences in the mesenteric LV architecture of ALCAM$^{-/-}$ as compared to WT mice (**Fig. 6*A***). While the overall tissue area covered by LVs was similar in both genotypes (data not shown), the LV network appeared to be more densely interconnected and less hierarchically organized in ALCAM$^{-/-}$ mice. This was reflected by a significant increase in the number of branching points (+55%, P=0.0005; Fig. 6*B*) and a significant increase in the number of ring-like structures formed by LVs (+29%, P=0.029; Fig.

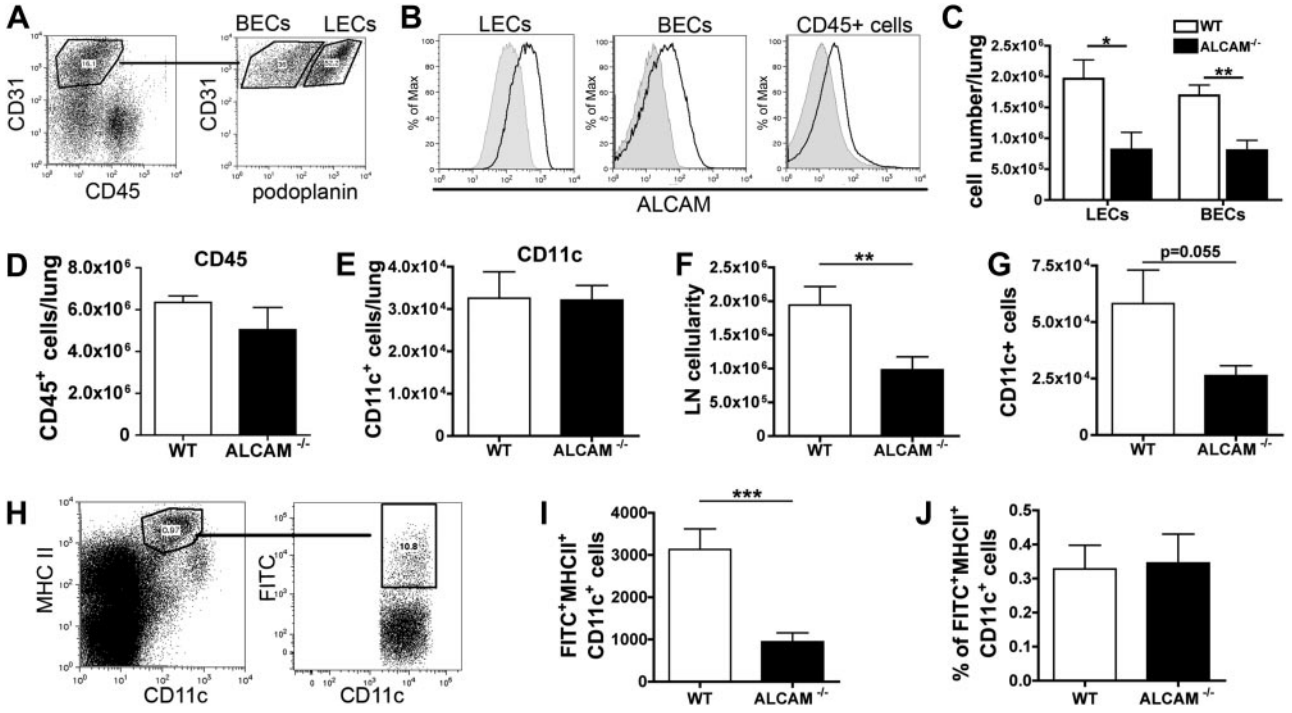

Figure 5. ALCAM is expressed in the lung vasculature and is important for DC migration. To investigate the expression of ALCAM on endothelial cells in murine lung tissue, single-cell suspensions generated from enzymatically digested mouse lungs were stained by FACS with antibodies against CD45, CD31, podoplanin, and ALCAM to differentiate between LECs ($CD45^-CD31^+podoplanin^+$), BECs ($CD45^-CD31^+podoplanin^-$), and leukocytes ($CD45^+CD31^-podoplanin^-$). *A*) Gating scheme. *B*) Analysis revealed that ALCAM was expressed in both lung LECs and BECs. Furthermore, ALCAM expression was also detected on $CD45^+$ cells. Black trace: candidate gene. Gray shaded trace: isotype control. *C*) FACS-based quantification revealed that LEC and BEC numbers were greatly reduced in the lungs of $ALCAM^{-/-}$ mice as compared to WT mice. *D, E*) By contrast, no significant reduction in the numbers of $CD45^+$ leukocytes ($P=0.95$; *D*) or of $CD11c^+$ ($P=0.33$; *E*) DCs was observed. Results from one experiment ($n=5$ mice/genotype) out of 3 similar experiments are shown (*C–E*). *F–J*) To study the effect of ALCAM deficiency on lymphatic vessel function, DC migration experiments were performed. $FITC^+$ latex beads were injected intratracheally, and bead-positive DCs were quantified in the lung dMLNs 24 h later. *F*) LN cellularity of the dMLNs was significantly reduced in $ALCAM^{-/-}$ as compared to WT mice. *G*) A near-significant reduction in the number of $CD11c^+$ DCs in MLNs was observed. *H*) Depiction of the gating scheme used to detect $CD11c^+MHCII^+FITC^+$ migratory DCs in dMLNs. *I, J*) The number of $CD11c^+MHCII^+FITC^+$ migratory DCs recovered from dMLNs was significantly reduced in $ALCAM^{-/-}$ as compared to WT mice (*I*), but the percentage of $CD11c^+MHCII^+FITC^+$ migratory DCs among all MLN cells was similar (*J*). Pooled data from 3 experiments ($n=15$ mice/genotype) are shown (*F–J*). $^*P < 0.05$; $^{**}P < 0.01$; $^{***}P < 0.001$.

6*C*). Furthermore, a subtle decrease in the average branch length (−9%, $P=0.043$; Fig. 6*D*) and in the average LV diameter (−10%, $P=0.16$; Fig. 6*E*) was observed. Somewhat surprisingly, the number of lymphatic valves, which were identified as areas of strongly positive Prox-1 staining, was increased in mesenteric LVs of $ALCAM^{-/-}$ as compared to WT mice (+ 23%, $P=0.06$; Fig. 6*F*).

In analogy to the mesentery, diaphragms collected from P6 $ALCAM^{-/-}$ and WT pups were also analyzed in whole-mount preparations. When staining for LYVE-1, major abnormalities in the LV network were observed (**Fig. 7**). Similarly to LVs found in the mesentery, LVs in the diaphragm formed an abnormally dense network, which was characterized by an increased number of branching points (+46%, $P=0.0016$; Fig. 7*B*). Furthermore, a striking increase in the organization of LVs into ring-like structures (+99%, $P=0.025$; Fig. 7*C*) was observed, indicative of a less hierarchical organization of the lymphatic vascular tree. Again, the overall tissue area covered by LVs was similar in both genotypes (data not shown), but LVs were significantly shorter and thinner in $ALCAM^{-/-}$ mice (−21%, $P=0.008$, and −15%; $P=0.014$, respectively; Fig. 7*D, E*). The number of blind-ended lymphatic initials appeared to be slightly reduced, but this was not significant (−18%, $P=0.24$; Fig. 7*F*).

In sum, our whole-mount data suggested that ALCAM deficiency prevented the formation of large LV with longer vessel segments and favored the formation of a more densely interconnected and less hierarchically organized LV network.

DISCUSSION

In this study, we have evaluated the expression of ALCAM in LECs and have identified a previously unknown role for this adhesion molecule in mediating the formation and function of the LV network.

Lymphangiogenesis, defined as the formation of new LVs, is characterized by distinct cellular processes, such

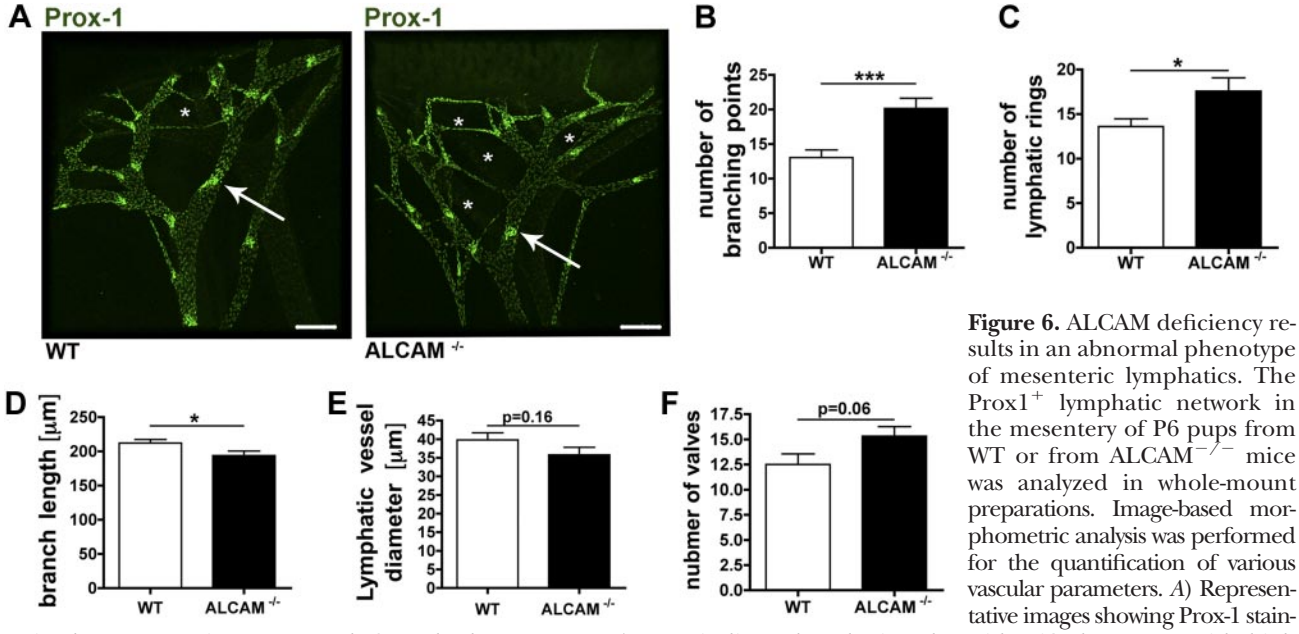

Figure 6. ALCAM deficiency results in an abnormal phenotype of mesenteric lymphatics. The Prox1$^+$ lymphatic network in the mesentery of P6 pups from WT or from ALCAM$^{-/-}$ mice was analyzed in whole-mount preparations. Image-based morphometric analysis was performed for the quantification of various vascular parameters. *A*) Representative images showing Prox-1 staining in the mesenteric LV network from both genotypes. Arrows indicate lymphatic valves, identified as areas with high accumulation of Prox-1$^+$ cells. Asterisks indicate ring-like LV structures. Scale bars = 200 µm. *B*) Total number of branching points was significantly increased in ALCAM$^{-/-}$ as compared to WT mice. *C*) Significantly more ring-like LV structures were present in the mesentery of ALCAM$^{-/-}$ as compared to WT mice. *D*, *E*) By contrast, the average branch length (*D*) and the lymphatic vessel diameter (*E*) were reduced. *F*) The number of valves was increased in ALCAM$^{-/-}$ as compared to WT mice. Pooled data obtained from 10 mice/group are shown. $^*P < 0.05$; $^{***}P < 0.001$.

as LEC proliferation, migration, and tube formation. Performing functional *in vitro* assays in presence of an ALCAM-blocking antibody or of an ALCAM-Fc fusion protein, we showed that LEC migration and tube formation, as well as LEC-LEC interactions were, at least in part, ALCAM-dependent. The latter findings suggest that the main role of ALCAM in LEC biology may lie in supporting the structural integrity and stability of LVs. Our findings that ALCAM strengthens interactions between neighboring cells are in agree-

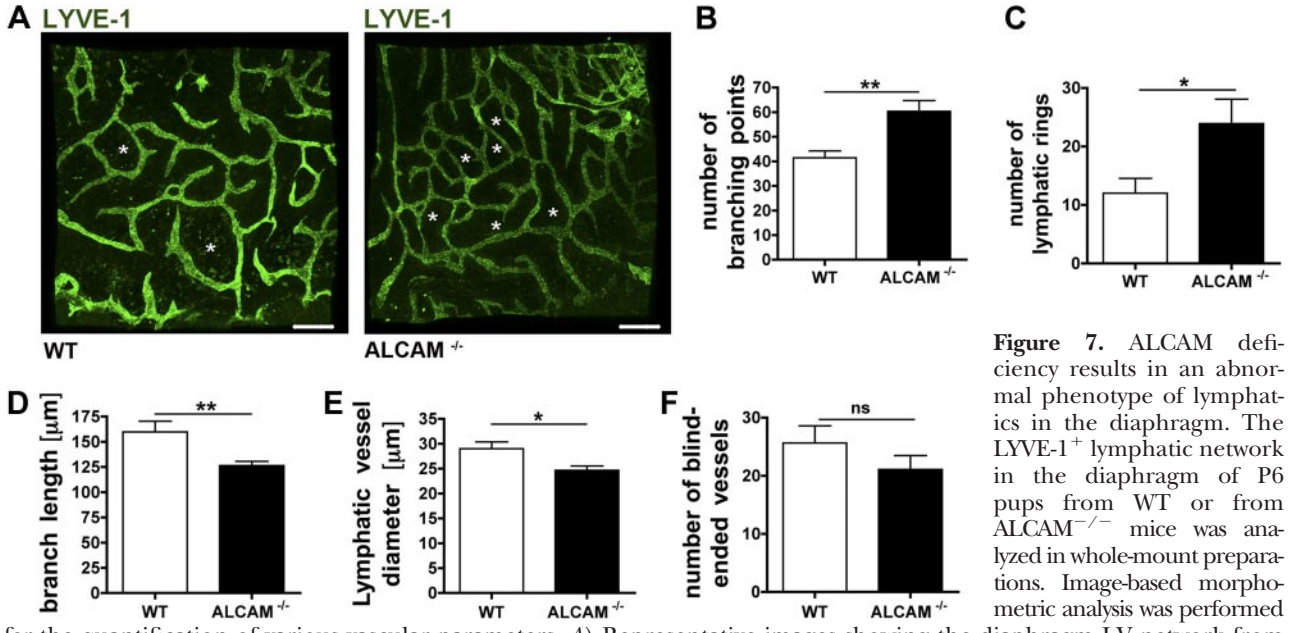

Figure 7. ALCAM deficiency results in an abnormal phenotype of lymphatics in the diaphragm. The LYVE-1$^+$ lymphatic network in the diaphragm of P6 pups from WT or from ALCAM$^{-/-}$ mice was analyzed in whole-mount preparations. Image-based morphometric analysis was performed for the quantification of various vascular parameters. *A*) Representative images showing the diaphragm LV network from both genotypes. Asterisks indicate ring-like LV structures. Scale bars = 200 µm. *B*) The total number of branching points was significantly increased in ALCAM$^{-/-}$ as compared to WT mice. *C*) Significantly more ring-like LV structures were present in the diaphragm of ALCAM$^{-/-}$ as compared to WT mice. *D*, *E*) By contrast, the average branch length (*D*) and lymphatic vessel diameter (*E*) were significantly reduced in ALCAM$^{-/-}$ as compared to WT mice. *F*) Numbers of blind-ended lymphatic initials were similar in ALCAM$^{-/-}$ as compared to WT mice. Pooled data obtained from 10 mice/group are shown. $^*P < 0.05$; $^{**}P < 0.01$.

ment with findings from the literature: ALCAM was initially shown to provide essential guidance and clustering cues for migrating neurons (28). Furthermore, ALCAM reportedly supports tube formation in BECs derived from the yolk sac (20). Moreover, various studies have demonstrated a role for ALCAM in tumor cell migration and clustering (14, 33). In fact, ALCAM is up-regulated in various tumors and, in certain tumor types, ALCAM up-regulation was shown to correlate with tumor progression and metastasis (14).

In agreement with our *in vitro* findings, we observed that the lymphatic network in the mesentery and in the diaphragm of ALCAM$^{-/-}$ mice displayed considerable morphological abnormalities. Specifically, LVs in ALCAM$^{-/-}$ mice appeared to be more densely interconnected. LVs were typically thinner than in WT mice and were preferentially arranged into ring-like structures, whereas LVs found in WT mice contained less branching points and formed part of a more hierarchically organized lymphatic network. This deficiency seemed to affect both lymphatic capillaries, visualized by LYVE-1 staining in the diaphragm, as well as lymphatic collectors, which constitute the main vessel type in the mesentery. During embryonic development, the formation of the lymphatic vascular system is initiated by the formation of primary lymph sacs, which arise from the anterior cardinal veins. From there, lymphatic vessels subsequently sprout to form a primary lymphatic capillary plexus (6, 34). Similar to the blood vascular system, the initial lymphatic network also undergoes further maturation and remodeling. This process, although not completely understood, involves the differentiation into initial and collecting LVs, but also the regression and fusion of preexisting vessels to generate a hierarchically organized LV network (6, 34). The phenotype observed in ALCAM$^{-/-}$ mice suggests that the absence of ALCAM compromised the formation or stabilization of larger LVs and their proper organization into a hierarchical LV network. Notably, defects in lymphatic network organization were already reported for mice deficient in Ang2 or in ephrinB2 (32, 35). However, in contrast to ALCAM deficiency, Ang2 or ephrinB2 deficiency also prevented the formation of lymphatic valves and resulted in a very severe lymphatic phenotype associated with postnatal lethality (32, 35, 36)

Interestingly, when analyzing the lung and LN vasculature of ALCAM$^{-/-}$ mice by quantitative FACS analysis, we observed that endothelial cell numbers were significantly reduced in these tissues and that this reduction correlated with ALCAM expression: While LECs in both tissues were ALCAM^{+}, and their numbers were significantly reduced in ALCAM$^{-/-}$ mice, BECs were only reduced in the lung but not in the LN, in agreement with ALCAM expression in lung BECs but not in LN BECs. The correlation of ALCAM expression with total LEC and BEC numbers in tissues could indicate a direct effect of ALCAM on endothelial cell proliferation. However, adding ALCAM-blocking Abs to *in vitro* cultured LECs did not affect LEC proliferation (data not shown). Therefore, it is rather perceivable that the reduction in numbers observed in ALCAM-deficient mice is caused by indirect effects, such as enhanced apoptosis of LECs in the absence of ALCAM, contributing to cell-cell interactions between adjacent LECs. Interestingly, in tumor cells, ALCAM was shown to be associated with the cytoskeleton, and ALCAM binding by its ligands induced intracellular signaling (37). Future studies will have to address whether ALCAM also induces cell signaling in endothelial cells. Besides engaging in homophilic interactions with neighboring ALCAM-expressing cells, it is possible that ALCAM also supports heterophilic interactions between LECs. In this regard, note that galectin-8, a small glycan-binding protein, was recently identified as a novel binding partner for ALCAM in human BECs (16). Furthermore, a previous study reported on the expression of galectin-8 in LECs and its role in LEC migration and adhesion (38). Thus, it is possible that heterophilic interactions between galectin-8 and ALCAM contribute to strengthening interactions between neighboring LECs. Similarly, the cell adhesion molecule L1CAM was recently identified as another ALCAM binding partner (15), and L1CAM was also shown to become up-regulated in LVs during inflammation (39).

Our analysis of the immune phenotype in ALCAM$^{-/-}$ mice revealed that leukocyte cell counts were only reduced in LNs and not in the spleen, demonstrating that loss of ALCAM does not lead to a general reduction of leukocytes in SLOs. Since LNs, in contrast to the spleen, contain afferent LVs, this finding additionally suggests that the reduced LN cellularity may be linked with the lymphatic phenotype observed in ALCAM$^{-/-}$ mice. Interestingly, in the thymus, a significant reduction in the number of single-positive CD4^{+} and CD8^{+} thymocytes was observed, indicating that ALCAM is involved in T-cell development. This finding is supported by previous reports demonstrating the expression of ALCAM on thymic epithelial cells (40) and a role for the ALCAM-ligand CD6 in thymocyte development (41).

Notably, ALCAM was previously shown to promote the migration of monocytes across BEC monolayers *in vitro* and across the blood brain barrier *in vivo* (21, 22). In line with the latter findings, we observed that blockade of ALCAM reduced the adhesion of DCs to LEC monolayers. However, our *in vivo* DC migration experiments did not reveal a role for DC-expressed ALCAM in DC migration to dLNs: Notably, when comparing DC migration in ALCAM$^{-/-}$ and WT mice, migration from the lung to dMLNs was similarly reduced for ALCAM^{+} and ALCAM^{-} DC populations. Thus, the reduction observed in DC migration in ALCAM$^{-/-}$ mice could not be explained by a loss of ALCAM-ALCAM interactions between DCs and LECs. Given that we observed marked morphological differences in LVs in the mesentery and in the diaphragm, as well as reduced LEC numbers in the lung, it is likely that also the LV network of the lung is compromised in ALCAM$^{-/-}$ mice. Over-

all, our findings suggest that the defect in DC migration observed in ALCAM$^{-/-}$ mice was due to morphological abnormalities in the LV network in absence of ALCAM. However, we cannot formally exclude that the reduced recovery of ALCAM$^{-/-}$ DCs from lung dMLNs was, at least in part, a consequence of the reduced MLN size in ALCAM$^{-/-}$ mice. On the other hand, it is well established that DCs arriving in LNs *via* the afferent lymph only migrate to the first dLN and are rarely found in efferent lymph (7). Thus, given the fact that DC numbers in the lung were comparable in ALCAM$^{-/-}$ and WT mice, it appears rather unlikely that the reduction in FITC^{+} DCs recovered from the dMLN is entirely explained by the reduced size of the MLN in ALCAM$^{-/-}$ mice. In fact, emerging studies have shown that the size and cellularity of LNs is regulated by DCs that have migrated to the LN *via* afferent LVs (42). Thus, it is perceivable that the correlation between DC migration and LN cellularity may rather be the opposite and that abnormalities in the lymphatic network and in DC migration actually account for the reduced LN cellularity observed in ALCAM$^{-/-}$ mice.

Although we detected ALCAM expression in peripheral organs like the lung, heart, or liver of mice, we could not detect ALCAM expression in the vasculature of the murine skin (data not shown). This was surprising, since we observed ALCAM expression in *in vitro* cultured human dermal LECs as well as in LVs in human skin. This finding indicates that species differences exist between ALCAM expression in mice and in humans. Notably, we (43) and others (10) have recently reported a similar species-dependent lymphatic expression pattern for the adhesion molecule CAR. Similar to ALCAM, CAR was expressed in LVs in human skin, but not in LVs in the murine skin (10, 43). Interestingly, a recent study by Mirza *et al.* (10) revealed that CAR is expressed in LVs in mouse embryonic skin, but becomes down-regulated in adulthood. It is therefore possible that ALCAM is also expressed in dermal lymphatics during mouse embryonic development and that its expression is lost once the dermal vasculature has developed. Intriguingly, we observed that *in vitro* cultured imLECs isolated from the skin of Immortomice (30) expressed ALCAM, indicating that ALCAM expression might be linked to endothelial cell activation or proliferation. In line with this hypothesis, ALCAM was recently found to be strongly up-regulated in the neovasculature in a murine lymphoma model (24). Furthermore, we and others (22) observed that ALCAM was up-regulated in LECs and BECs in response to inflammatory cytokines. Taken together, it seems that ALCAM is expressed in the vasculature in a species- and tissue-specific manner and that its expression may be further modulated under conditions of endothelial cells activation, such as inflammation or tumor growth.

Collectively, our data reveal a novel role for ALCAM in stabilizing LEC-LEC interactions and in the organization and function of the LV network. Finally, our findings suggest that blockade of ALCAM could be a therapeutic approach for inhibiting lymphangiogenesis in pathological conditions. FJ

The authors thank Csaba Balazs (ETH Zurich) for developing the ImageJ-based script used for image quantification and Simone Haener (ETH Zurich) for excellent technical support. Furthermore, the authors thank Joshua Weiner (University of Iowa, Iowa City, IA, USA) for providing tissue samples of ALCAM$^{-/-}$ and control mice in the beginning of the project. C.H, gratefully acknowledges financial support from the Swiss National Fund (grant 310030_138330), the Prof. Dr. Max Cloëtta Foundation, and ETH Zurich (project grant 0-20566_09). M.I. designed research, performed research, analyzed data, and wrote the paper; S.K., A.H.W., and S.W. performed research and analyzed and discussed data; C.H. designed research, analyzed data, and wrote the paper. The authors declare no conflicts of interest.

REFERENCES

1. Vestweber, D. (2012) Relevance of endothelial junctions in leukocyte extravasation and vascular permeability. *Ann. N. Y. Acad. Sci.* **1257,** 184–192
2. Garrido-Urbani, S., Bradfield, P. F., Lee, B. P., and Imhof, B. A. (2008) Vascular and epithelial junctions: a barrier for leucocyte migration. *Biochem. Soc. Trans.* **36,** 203–211
3. Ishida, T., Kundu, R. K., Yang, E., Hirata, K., Ho, Y. D., and Quertermous, T. (2003) Targeted disruption of endothelial cell-selective adhesion molecule inhibits angiogenic processes in vitro and in vivo. *J. Biol. Chem.* **278,** 34598–34604
4. Avraamides, C. J., Garmy-Susini, B., and Varner, J. A. (2008) Integrins in angiogenesis and lymphangiogenesis. *Nat. Rev. Cancer* **8,** 604–617
5. Yan, X., Lin, Y., Yang, D., Shen, Y., Yuan, M., Zhang, Z., Li, P., Xia, H., Li, L., Luo, D., Liu, Q., Mann, K., and Bader, B. L. (2003) A novel anti-CD146 monoclonal antibody, AA98, inhibits angiogenesis and tumor growth. *Blood* **102,** 184–191
6. Schulte-Merker, S., Sabine, A., and Petrova, T. V. (2011) Lymphatic vascular morphogenesis in development, physiology, and disease. *J. Cell. Biol.* **193,** 607–618
7. Forster, R., Braun, A., and Worbs, T. (2012) Lymph node homing of T cells and dendritic cells via afferent lymphatics. *Trends Immunol.* **33,** 271–280
8. Pfeiffer, F., Kumar, V., Butz, S., Vestweber, D., Imhof, B. A., Stein, J. V., and Engelhardt, B. (2008) Distinct molecular composition of blood and lymphatic vascular endothelial cell junctions establishes specific functional barriers within the peripheral lymph node. *Eur. J. Immunol.* **38,** 2142–2155
9. Pflicke, H., and Sixt, M. (2009) Preformed portals facilitate dendritic cell entry into afferent lymphatic vessels. *J. Exp. Med.* **206,** 2925–2935
10. Mirza, M., Pang, M. F., Zaini, M. A., Haiko, P., Tammela, T., Alitalo, K., Philipson, L., Fuxe, J., and Sollerbrant, K. (2012) Essential role of the Coxsackie and adenovirus receptor (CAR) in development of the lymphatic system in mice. *PLoS One* **7,** e37523
11. Bazigou, E., Lyons, O. T., Smith, A., Venn, G. E., Cope, C., Brown, N. A., and Makinen, T. (2011) Genes regulating lymphangiogenesis control venous valve formation and maintenance in mice. *J. Clin. Invest.* **121,** 2984–2992
12. Garmy-Susini, B., Avraamides, C. J., Schmid, M. C., Foubert, P., Ellies, L. G., Barnes, L., Feral, C., Papayannopoulou, T., Lowy, A., Blair, S. L., Cheresh, D., Ginsberg, M., and Varner, J. A. (2010) Integrin alpha4beta1 signaling is required for lymphangiogenesis and tumor metastasis. *Cancer Res.* **70,** 3042–3051
13. Van Kempen, L. C., Nelissen, J. M., Degen, W. G., Torensma, R., Weidle, U. H., Bloemers, H. P., Figdor, C. G., and Swart, G. W. (2001) Molecular basis for the homophilic activated leukocyte cell adhesion molecule (ALCAM)-ALCAM interaction. *J. Biol. Chem.* **276,** 25783–25790
14. Weidle, U. H., Eggle, D., Klostermann, S., and Swart, G. W. (2010) ALCAM/CD166: cancer-related issues. *Cancer Genomics Proteomics* **7,** 231–243

15. Buhusi, M., Demyanenko, G. P., Jannie, K. M., Dalal, J., Darnell, E. P., Weiner, J. A., and Maness, P. F. (2009) ALCAM regulates mediolateral retinotopic mapping in the superior colliculus. *J. Neurosci.* **29,** 15630–15641
16. Delgado, V. M., Nugnes, L. G., Colombo, L. L., Troncoso, M. F., Fernandez, M. M., Malchiodi, E. L., Frahm, I., Croci, D. O., Compagno, D., Rabinovich, G. A., Wolfenstein-Todel, C., and Elola, M. T. (2011) Modulation of endothelial cell migration and angiogenesis: a novel function for the "tandem-repeat" lectin galectin-8. *FASEB J.* **25,** 242–254
17. Zimmerman, A. W., Joosten, B., Torensma, R., Parnes, J. R., van Leeuwen, F. N., and Figdor, C. G. (2006) Long-term engagement of CD6 and ALCAM is essential for T-cell proliferation induced by dendritic cells. *Blood* **107,** 3212–3220
18. Van Kempen, L. C., van den Oord, J. J., van Muijen, G. N., Weidle, U. H., Bloemers, H. P., and Swart, G. W. (2000) Activated leukocyte cell adhesion molecule/CD166, a marker of tumor progression in primary malignant melanoma of the skin. *Am. J. Pathol.* **156,** 769–774
19. Ohneda, O., Ohneda, K., Arai, F., Lee, J., Miyamoto, T., Fukushima, Y., Dowbenko, D., Lasky, L. A., and Suda, T. (2001) ALCAM (CD166): its role in hematopoietic and endothelial development. *Blood* **98,** 2134–2142
20. Ikeda, K., and Quertermous, T. (2004) Molecular isolation and characterization of a soluble isoform of activated leukocyte cell adhesion molecule that modulates endothelial cell function. *J. Biol. Chem.* **279,** 55315–55323
21. Masedunskas, A., King, J. A., Tan, F., Cochran, R., Stevens, T., Sviridov, D., and Ofori-Acquah, S. F. (2006) Activated leukocyte cell adhesion molecule is a component of the endothelial junction involved in transendothelial monocyte migration. *FEBS Lett.* **580,** 2637–2645
22. Cayrol, R., Wosik, K., Berard, J. L., Dodelet-Devillers, A., Ifergan, I., Kebir, H., Haqqani, A. S., Kreymborg, K., Krug, S., Moumdjian, R., Bouthillier, A., Becher, B., Arbour, N., David, S., Stanimirovic, D., and Prat, A. (2008) Activated leukocyte cell adhesion molecule promotes leukocyte trafficking into the central nervous system. *Nat. Immunol.* **9,** 137–145
23. Ofori-Acquah, S. F., King, J., Voelkel, N., Schaphorst, K. L., and Stevens, T. (2008) Heterogeneity of barrier function in the lung reflects diversity in endothelial cell junctions. *Microvasc. Res.* **75,** 391–402
24. Schliemann, C., Roesli, C., Kamada, H., Borgia, B., Fugmann, T., Klapper, W., and Neri, D. (2010) In vivo biotinylation of the vasculature in B-cell lymphoma identifies BST-2 as a target for antibody-based therapy. *Blood* **115,** 736–744
25. Hirakawa, S., Hong, Y. K., Harvey, N., Schacht, V., Matsuda, K., Libermann, T., and Detmar, M. (2003) Identification of vascular lineage-specific genes by transcriptional profiling of isolated blood vascular and lymphatic endothelial cells. *Am. J. Pathol.* **162,** 575–586
26. Halin, C., and Detmar, M. (2008) Chapter 1. Inflammation, angiogenesis, and lymphangiogenesis. *Methods Enzymol.* **445,** 1–25
27. Geback, T., Schulz, M. M., Koumoutsakos, P., and Detmar, M. (2009) TScratch: a novel and simple software tool for automated analysis of monolayer wound healing assays. *BioTechniques* **46,** 265–274
28. Weiner, J. A., Koo, S. J., Nicolas, S., Fraboulet, S., Pfaff, S. L., Pourquie, O., and Sanes, J. R. (2004) Axon fasciculation defects and retinal dysplasias in mice lacking the immunoglobulin superfamily adhesion molecule BEN/ALCAM/SC1. *Mol. Cell. Neurosci.* **27,** 59–69
29. Karkkainen, M. J., Haiko, P., Sainio, K., Partanen, J., Taipale, J., Petrova, T. V., Jeltsch, M., Jackson, D. G., Talikka, M., Rauvala, H., Betsholtz, C., and Alitalo, K. (2004) Vascular endothelial growth factor C is required for sprouting of the first lymphatic vessels from embryonic veins. *Nat. Immunol.* **5,** 74–80
30. Vigl, B., Aebischer, D., Nitschke, M., Iolyeva, M., Rothlin, T., Antsiferova, O., and Halin, C. (2011) Tissue inflammation modulates gene expression of lymphatic endothelial cells and dendritic cell migration in a stimulus-dependent manner. *Blood* **118,** 205–215
31. Jakubzick, C., and Randolph, G. J. (2010) Methods to study pulmonary dendritic cell migration. *Methods Mol. Biol.* **595,** 371–382
32. Makinen, T., Adams, R. H., Bailey, J., Lu, Q., Ziemiecki, A., Alitalo, K., Klein, R., and Wilkinson, G. A. (2005) PDZ interaction site in ephrinB2 is required for the remodeling of lymphatic vasculature. *Genes Dev.* **19,** 397–410
33. Ofori-Acquah, S. F., and King, J. A. (2008) Activated leukocyte cell adhesion molecule: a new paradox in cancer. *Translational Res. J. Lab. Clin. Med.* **151,** 122–128
34. Oliver, G. (2004) Lymphatic vasculature development. *Nat. Rev. Immunol.* **4,** 35–45
35. Gale, N. W., Thurston, G., Hackett, S. F., Renard, R., Wang, Q., McClain, J., Martin, C., Witte, C., Witte, M. H., Jackson, D., Suri, C., Campochiaro, P. A., Wiegand, S. J., and Yancopoulos, G. D. (2002) Angiopoietin-2 is required for postnatal angiogenesis and lymphatic patterning, and only the latter role is rescued by angiopoietin-1. *Dev. Cell* **3,** 411–423
36. Dellinger, M., Hunter, R., Bernas, M., Gale, N., Yancopoulos, G., Erickson, R., and Witte, M. (2008) Defective remodeling and maturation of the lymphatic vasculature in Angiopoietin-2 deficient mice. *Dev. Biol.* **319,** 309–320
37. Swart, G. W., Lunter, P. C., Kilsdonk, J. W., and Kempen, L. C. (2005) Activated leukocyte cell adhesion molecule (ALCAM/CD166): signaling at the divide of melanoma cell clustering and cell migration? *Cancer Metastasis Rev.* **24,** 223–236
38. Cueni, L. N., and Detmar, M. (2009) Galectin-8 interacts with podoplanin and modulates lymphatic endothelial cell functions. *Exp. Cell Res.* **315,** 1715–1723
39. Maddaluno, L., Verbrugge, S. E., Martinoli, C., Matteoli, G., Chiavelli, A., Zeng, Y., Williams, E. D., Rescigno, M., and Cavallaro, U. (2009) The adhesion molecule L1 regulates transendothelial migration and trafficking of dendritic cells. *J. Exp. Med.* **206,** 623–635
40. Patel, D. D., Wee, S. F., Whichard, L. P., Bowen, M. A., Pesando, J. M., Aruffo, A., and Haynes, B. F. (1995) Identification and characterization of a 100-kD ligand for CD6 on human thymic epithelial cells. *J. Exp. Med.* **181,** 1563–1568
41. Singer, N. G., Fox, D. A., Haqqi, T. M., Beretta, L., Endres, J. S., Prohaska, S., Parnes, J. R., Bromberg, J., and Sramkoski, R. M. (2002) CD6: expression during development, apoptosis and selection of human and mouse thymocytes. *Int. Immunol.* **14,** 585–597
42. Girard, J. P., Moussion, C., and Forster, R. (2012) HEVs, lymphatics and homeostatic immune cell trafficking in lymph nodes. *Nat. Rev. Immunol.* **12,** 762–773
43. Vigl, B., Zgraggen, C., Rehman, N., Banziger-Tobler, N. E., Detmar, M., and Halin, C. (2009) Coxsackie- and adenovirus receptor (CAR) is expressed in lymphatic vessels in human skin and affects lymphatic endothelial cell function in vitro. *Exp. Cell Res.* **315,** 336–347

Received for publication August 1, 2012.
Accepted for publication November 5, 2012.